Acta Crystallographica Section F
**Structural Biology and Crystallization Communications**
ISSN 1744-3091

# Crystallization and preliminary crystallographic studies of both components of the staphylococcal LukE–LukD leukotoxin

**Romain Galy,[a,b] Fabien Bergeret,[a,b] Daniel Keller,[c] Lionel Mourey,[a,b] Gilles Prévost[c] and Laurent Maveyraud[a,b]***

[a]Institut de Pharmacologie et de Biologie Structurale (IPBS), Centre National de la Recherche Scientifique (CNRS), 205 Route de Narbonne, BP 64182, F-31077 Toulouse, France, [b]Université de Toulouse, Université Paul Sabatier, IPBS, F-31077 Toulouse, France, and [c]Physiopathologie Cellulaire – Université de Strasbourg, Hôpitaux Universitaires de Strasbourg, Institut de Bactériologie, 3 Rue Koeberlé, F-67000 Strasbourg, France

Correspondence e-mail: laurent.maveyraud@ipbs.fr

Received 5 March 2012
Accepted 4 April 2012

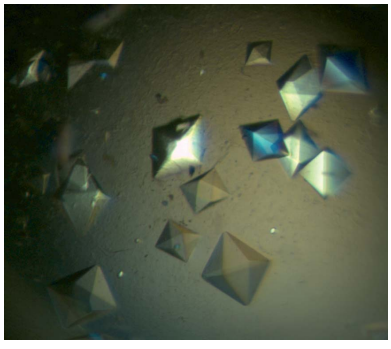



Soluble forms of recombinant LukE protein (expressed in *Escherichia coli*) and of wild-type LukD protein (expressed in *Staphylococcus aureus*), which together form the staphylococcal LukE–LukD leukotoxin, were purified to homogeneity and crystallized using the sitting-drop vapour-diffusion method. The crystals of LukE belonged to space group $I4$, with unit-cell parameters $a = b = 134.50$, $c = 64.43$ Å, and diffracted X-rays to 1.6 Å resolution. The crystals of LukD belonged to space group $P2_12_12_1$, with unit-cell parameters $a = 48.04$, $b = 50.99$, $c = 137.40$ Å, and diffracted to 1.9 Å resolution. Molecular replacement using the LukF-PV structure (PDB entry 1pvl) as a template model allowed the identification of an initial structure solution for the LukD data. In the case of LukE, a solution comprising only a single copy of the search model (LukS-PV; PDB entry 1t5r) was found, although the unit-cell parameters indicated that up to three molecules could be accommodated in the asymmetric unit.

## 1. Introduction

Among the numerous virulence factors expressed by *Staphylococcus aureus*, leukotoxins are able to form pores across the membranes of leukocytes and therefore to alter the host immune defences (Diep *et al.*, 2010). To date, eight leukotoxins have been identified from *S. aureus* strains: α-haemolysin (Gray & Kehoe, 1984), Panton and Valentine leukocidin (PVL, composed of LukS-PV and LukF-PV; Woodin, 1960), two γ-haemolysins (HlgA–HlgB and HlgC–HlgB; Cooney *et al.*, 1993; Prévost, Cribier *et al.*, 1995), LukM–LukF′-PV (Kaneko *et al.*, 1997), LukE–LukD (Gravet *et al.*, 1998), LukEv–LukDv (Morinaga *et al.*, 2003) and, more recently, LukH–LukG (Ventura *et al.*, 2010). *S. intermedius* has been also reported to express a leukotoxin, LukS-I–LukF-I (Prévost, Bouakham *et al.*, 1995). These toxins are related to cutaneous infections (Prévost, Couppié *et al.*, 1995), such as furuncles (Baba-Moussa *et al.*, 2011), dermonecroses and abscesses (Lina *et al.*, 1999), and also to pulmonary infections and inflammatory reactions (Girgis *et al.*, 2005; Prévost, Cribier *et al.*, 1995).

With the notable exception of α-haemolysin, which acts as a homoheptamer (Gouaux *et al.*, 1994), leukotoxins are composed of two distinct proteins, one of class S (related to the slow-eluted component of PVL) and one of class F (related to the fast-eluted component of PVL); leukotoxin protomers are secreted as soluble proteins. The names of the bipartite leukotoxins start with the S component, which is followed by the F component. The toxic action of leukotoxins is exerted in a three-step mechanism: binding of the S component to the target cell membrane and subsequent recruitment of the F component (Meyer *et al.*, 2009), oligomerization into a prepore and, eventually, the formation of a pore across the cell membrane, resulting in cell lysis (Fig. 1). Independently of pore formation, leukotoxins are able to rapidly activate cellular signalling pathways (Baba-Moussa *et al.*, 1999), including calcium release and chemokine secretion (Tseng *et al.*, 2009).

Leukotoxin components contain between 280 and 301 residues. The class S components, with the exception of LukH, display 63–76% sequence identity, whereas the class F components, with the exception of LukG, share 69–83% sequence identity. When LukH or LukG are included in the comparison, the sequence-identity levels drop to

about 30–34%. Similarities across classes are much weaker, ranging from 22 to 30% sequence identity, or even below 20% when F and S proteins are compared with α-haemolysin. Upon exerting their toxic role, leukotoxin components have to face either a hydrophilic environment when secreted at the infection site or a hydrophobic medium when inserted into the target cell membrane. The structures of soluble forms of the S [LukS-PV (Guillet *et al.*, 2004) and HlgA (Roblin *et al.*, 2008)] and F [LukF-PV (Pédelacq *et al.*, 1999) and HlgB (Olson *et al.*, 1999; Roblin *et al.*, 2008)] components of Luk-PV and HlgB–HlgA indicate that they are built of three distinct domains: a central domain made of a β-sandwich of two six-stranded antiparallel β-sheets, a stem domain built of three β-strands closely packed to the central domain and a rim domain consisting of four antiparallel β-strands, two α-helices and two loops. This rim domain is likely to be responsible for interaction with the membrane. Upon pore formation, the stem domain extends from the central domain and deploys two long antiparallel β-strands that insert into the membrane and become part of the β-barrel (Song *et al.*, 1996; Yamashita *et al.*, 2011). For bipartite leukotoxins the pore is likely to be octameric, with alternating S and F components (Joubert *et al.*, 2006; Viero *et al.*, 2006; Yamashita *et al.*, 2011). The three-dimensional structure of the octameric pore formed by HlgA and HlgB (Yamashita *et al.*, 2011), as well as a model of the pre-pore of PVL (Aman *et al.*, 2010), has recently been reported. A mechanism of pore formation has also been proposed for HlgA–HlgB (Yamashita *et al.*, 2011), which is the only known leukotoxin that is able to form a pore in a synthetic membrane, but its pertinence to other leukotoxins remains to be confirmed.

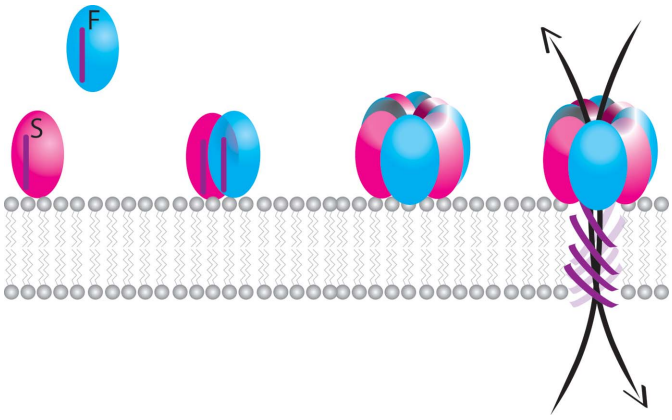


**Figure 1**
Schematic mechanism of pore formation by two-component leukotoxins. (*a*) Binding of the S component to the target cell membrane, which may require the presence of a specific receptor, (*b*) recruitment of the F component, (*c*) oligomerization into an octameric prepore and (*d*) stem deployment and pore formation. The purple bar represents the stem domain, which is packed against the β-sandwich domain in the soluble forms of the proteins.

Although the LukE–LukD leukotoxin has been shown to be expressed by up to two thirds of *S. aureus* isolates (Arciola *et al.*, 2007) and may contribute to the bloodstream virulence of *S. aureus* (Alonzo *et al.*, 2012), no specific clinical association has been reported. However, its expression has frequently been found in strains responsible for bullous impetigo (Gravet *et al.*, 2001) and diarrhoea (Gravet *et al.*, 1999). Here, we report the expression, purification and crystallization of both the LukE and the LukD components.

## 2. Materials and methods

### 2.1. Expression and purification

LukD was purified from *S. aureus* strain N65 (ΔHlg) (Supersac *et al.*, 1998) according to a protocol derived from Finck-Barbançon *et al.* (1991). A single colony was grown for 15 h at 310 K in YCP medium (30 g $l^{-1}$ yeast extract, 20 g $l^{-1}$ casamino acids, 20 g $l^{-1}$ sodium pyruvate, 2.5 g $l^{-1}$ $Na_2HPO_4$, 0.4 g $l^{-1}$ $KH_2PO_4$, pH 7.0). Solid ammonium sulfate was added to the supernatant of the cell culture to 80% saturation at pH 7.0 and 277 K. The precipitate was dissolved in water, dialyzed extensively against 30 m*M* sodium phosphate buffer pH 6.5 (buffer 1) and loaded onto an SP Sepharose Fast Flow column. The column was extensively washed with buffer 1 and proteins were directly eluted with buffer 1 supplemented with 700 m*M* NaCl. After dialysis against buffer 1, the fractions containing LukD were loaded onto a Resource S column and elution was performed with a linear gradient of NaCl (0–400 m*M*) in buffer 1. Fractions containing LukD were supplemented with ammonium sulfate to a final concentration of 1.6 *M* and loaded onto a Source 15 ISO column. Proteins were eluted with a decreasing gradient of ammonium sulfate (1600–600 m*M*). After extensive dialysis against buffer 1, fractions containing LukD were loaded onto a Mono S 10/100 GL column and eluted with a gradient of NaCl (0–200 m*M*).

The gene encoding LukE from *S. aureus* strain N65 was cloned into the *Eco*RI site of pGEX6P-1 and transformed into *Escherichia coli*

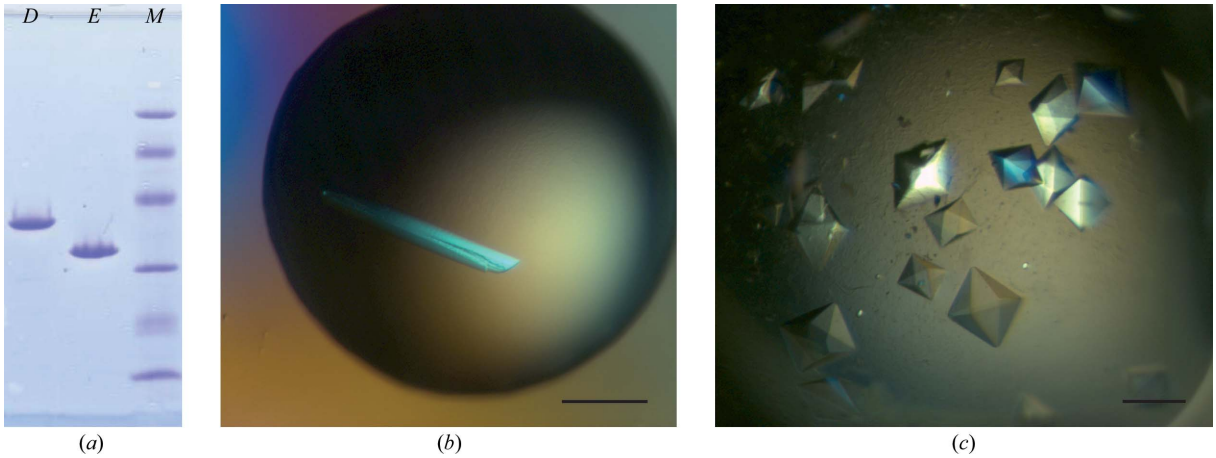


(*a*) (*b*) (*c*)

**Figure 2**
(*a*) SDS–PAGE analysis with Coomassie Blue staining. Lane *D*, LukD; lane *E*, LukE, lane *M*, molecular-weight markers (from top to bottom: 94, 67, 43, 30, 20.1 and 14.4 kDa). (*b*) Crystals of LukE. (*c*) Crystals of LukD. The scale bar in (*b*) and (*c*) corresponds to 100 µm.

BL21 cells. Cells were grown in TYA medium (17 g $l^{-1}$ tryptone, 10 g $l^{-1}$ yeast extract, 5 g $l^{-1}$ NaCl, 15 g $l^{-1}$ bacto agar, 100 mg $l^{-1}$ ampicillin) at 310 K until an OD of 0.5–1.0 was reached. Expression of the GST-LukE fusion protein was induced with 0.2 m*M* IPTG and continued for 15 h at 303 K. Cells were collected and lysed in buffer 2 (30 m*M* HEPES, 150 m*M* NaCl, 1 m*M* EDTA pH 7.2) at 76 MPa with a French press. The supernatant was loaded onto a Glutathione Sepharose 4B column, which was eluted with 30 m*M* reduced gluthathione, 500 m*M* NaCl, 50 m*M* Tris–HCl pH 8.0. Cleavage of the GST was performed for 15 h at 277 K with 20 units of PreScission protease (GE Healthcare). After dialysis against 50 m*M* HEPES, 100 m*M* NaCl pH 7.5, a final purification step was performed on a Resource S column eluted with a gradient of NaCl (130–260 m*M*).

Proteins were characterized using SDS–PAGE (Fig. 2*a*) and radial immunoprecipitation using purified specific rabbit antibodies.

### 2.2. Crystallization

Dynamic light scattering was used to determine the most appropriate conditioning buffer with respect to the monodispersity of the solution. Both proteins were conditioned in 50 m*M* MES pH 6.0, 50 m*M* NaCl using Vivaspin ultrafiltration devices (10 kDa cutoff, Sartorius) and were concentrated to about 10 mg $ml^{-1}$ as evaluated using the sequence-derived molar extinction coefficient. Crystallization conditions were identified using commercial kits from Qiagen (JCSG Core I–IV, Classics, pH Clear, pH Clear II, $AmSO_4$, PEGs and PEGs II Suites). Sitting drops were formed by mixing 150 nl protein solution with 150 nl reservoir solution using a NanoDrop ExtY crystallization robot (Innovadyne) at 285 K. The reservoir volume was 70 µl.

### 2.3. Data collection and processing

Cryoprotection was achieved by soaking LukE or LukD crystals for 2 min in the crystallization solution supplemented with 20% ethylene glycol prior to transfer into a gaseous nitrogen flow at 100 K. Data were collected from LukE crystals to 1.65 Å resolution (Fig. 3*a*) on the ID29 beamline at the European Synchrotron Radiation Facility (ESRF, Grenoble, France) with a wavelength of 0.9756 Å using a Quantum 315 CCD detector (ADSC, USA). 180 oscillations of 1° were collected with an exposure time of 3.0 s. The crystal-to-detector distance was set to 190 mm.

LukD crystals were irradiated on the ID23-EH2 beamline at the ESRF with a wavelength of 0.8726 Å. Diffracted intensities were collected to 1.90 Å resolution (Fig. 3*b*) using a MAR CCD detector (MAR Research, Germany). The crystal-to-detector distance was set to 237.5 mm and 180 images were collected with an oscillation angle of 1° and an exposure time of 2.0 s.

Data processing was initially performed using *autoPROC* (Vonrhein *et al.*, 2011) and was optimized with *XDS* (Kabsch, 2010) and *SCALA* (Evans, 2006). All subsequent operations were performed using the *CCP*4 program suite (Winn *et al.*, 2011).

Molecular replacement was performed using *Phaser* v.2.3 (McCoy *et al.*, 2007) as distributed in the *CCP*4 v.6.1 program suite. The structures of the PVL components were used as models: LukF-PV (PDB entry 1pvl; Pédelacq *et al.*, 1999) was used for LukD (sequence identity of 73%) and LukS-PV (PDB entry 1t5r; Guillet *et al.*, 2004) was used in the case of LukE (sequence identity of 64%). The starting models were reduced to polyalanine, except for conserved residues, for which the full side chains were preserved. The molecular-replacement search was performed for all possible enantiomorphic space groups in each case.

## 3. Results and discussion

About 3 mg pure LukD protein could be purified starting from 2.4 l *S. aureus* culture. During the final chromatographic step, two peaks containing LukD were obtained. These peaks, which contained 35% and 65% of the total LukD, eluted at NaCl concentrations of 180 and 200 m*M*, respectively. Based on our previous experiments with other

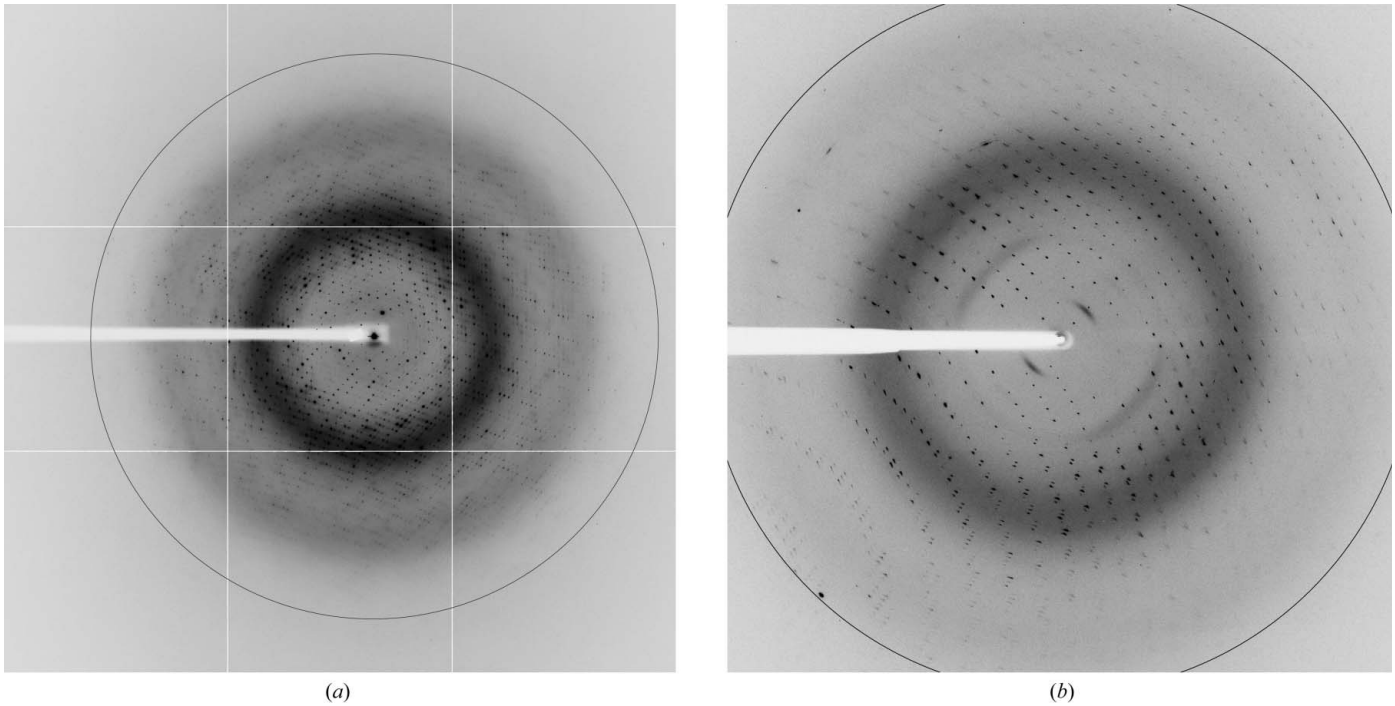

(*a*) (*b*)

**Figure 3**
X-ray diffraction patterns collected from (*a*) a LukE crystal and (*b*) a LukD crystal. The circles correspond to the limits of diffraction: 1.65 Å in (*a*) and 1.90 Å in (*b*).

**Table 1**
Data-collection statistics for LukE and LukD crystals.

Values in parentheses are for the highest resolution shell.

| | LukE | LukD |
|---|---|---|
| Beamline | ID29, ESRF | ID23-EH2, ESRF |
| Wavelength | 0.9756 | 0.8726 |
| Space group | *I*4 | $P2_12_12_1$ |
| Unit-cell parameters (Å) | $a = b = 134.90$, $c = 64.13$ | $a = 48.04$, $b = 50.99$, $c = 137.40$ |
| Resolution range (Å) | 36.82–1.65 (1.74–1.65) | 34.97–1.90 (2.00–1.90) |
| Observed reflections | 507974 (72890) | 138442 (7810) |
| Unique reflections | 69188 (10065) | 25099 (2609) |
| Multiplicity | 7.3 (7.2) | 5.5 (3.0) |
| Completeness (%) | 99.9 (100.0) | 91.3 (66.6) |
| $\langle I/\sigma(I)\rangle$ | 16.7 (3.1) | 15.0 (2.4) |
| $R_{\rm merge}$ | 0.066 (0.639) | 0.077 (0.403) |

leukotoxins, the first peak was likely to correspond to partial proteolysis of LukD and was discarded. In the case of LukE, the yield of pure protein was about 10 mg per litre of culture. In addition to the 286 residues of LukE, the purified protein also includes eight residues at the N-terminus, GPLGSPEF, which remained from the PreScission cleavage site.

LukE crystals were observed after two weeks in conditions consisting of 20%(*w*/*v*) polyethylene glycol (PEG) 3350 with various salts at 0.2 *M*. The best diffracting crystals were obtained with ammonium acetate, corresponding to condition No. 83 of the PEGs Suite (Fig. 2*b*). LukD crystals were observed after four weeks in 30% PEG 4000, 0.1 *M* Tris–HCl pH 8.5, 0.2 *M* lithium sulfate, corresponding to condition No. 45 of the PEGs II Suite (Fig. 2*c*).

Data-processing statistics are given in Table 1. The LukE crystals belonged to the tetragonal space group *I*4, with unit-cell parameters $a = b = 134.90$, $c = 64.13$ Å. The LukD crystals were orthorhombic, with unit-cell parameters $a = 48.04$, $b = 50.99$, $c = 137.40$ Å; analysis of the systematic absences suggested the space group to be $P2_12_12_1$.

The unit-cell parameters of LukD crystals allow the presence of only one molecule per asymmetric unit, with a Matthews coefficient of 2.41 Å$^3$ Da$^{-1}$ and a solvent content of 49%. The situation is less clear-cut in the case of LukE, since up to three molecules per asymmetric unit can be accommodated. The Matthews coefficient calculated for two molecules per asymmetric unit was 2.26 Å$^3$ Da$^{-1}$, with a solvent content of 46%. Given the Matthews coefficient value and the resolution limit of 1.9 Å, this was considered to be the most probable cell content (Kantardjieff & Rupp, 2003). However, neither the self-rotation function nor the self-Patterson function suggested the existence of noncrystallographic symmetry.

A clear unique solution was identified in space group $P2_12_12_1$ for LukD, with a rotation-function *Z* score of 14.8 and a translation-function *Z* score of 37.7. In the case of LukE, up to two copies were searched for in the asymmetric unit. However, only one molecule could be located, with *Z* scores of 20.9 for the rotation function and 44.0 for the translation function. Attempts to localize a second copy of the model remained unsuccessful. Indeed, the presence of a second molecule was systematically rejected by the packing-function violation criteria.

Refinement of these molecular-replacement solutions are currently in progress and structural details will be presented in a separate paper.

This project was supported by the Centre National de la Recherche Scientifique (CNRS). RG is supported by a fellowship from the Scientific Council of the Université Paul Sabatier, Université de Toulouse. The 'Direction de la Recherche et des Etudes Doctorales' of the Université de Strasbourg is acknowledged for financial support (EA-4438 – Physiopathologie et Médecine Translationnelle). Crystallization experiments were performed at the Integrated Screening Platform of Toulouse (PICT, IBISA).

## References

Alonzo, F., Benson, M. A., Chen, J., Novick, R. P., Shopsin, B. & Torres, V. J. (2012). *Mol. Microbiol.* **83**, 423–435.
Aman, M. J., Karauzum, H., Bowden, M. G. & Nguyen, T. L. (2010). *J. Biomol. Struct. Dyn.* **28**, 1–12.
Arciola, C. R., Baldassarri, L., Von Eiff, C., Campoccia, D., Ravaioli, S., Pirini, V., Becker, K. & Montanaro, L. (2007). *Int. J. Artif. Organs*, **30**, 792–797.
Baba-Moussa, L., Sina, H., Scheftel, J.-M., Moreau, B., Sainte-Marie, D., Kotchoni, S. O., Prévost, G. & Couppié, P. (2011). *PLoS One*, **6**, e25716.
Baba Moussa, L., Werner, S., Colin, D. A., Mourey, L., Pédelacq, J.-D., Samama, J.-P., Sanni, A., Monteil, H. & Prévost, G. (1999). *FEBS Lett.* **461**, 280–286.
Cooney, J., Kienle, Z., Foster, T. J. & O'Toole, P. W. (1993). *Infect. Immun.* **61**, 768–771.
Diep, B. A. *et al.* (2010). *Proc. Natl Acad. Sci. USA*, **107**, 5587–5592.
Evans, P. (2006). *Acta Cryst.* D**62**, 72–82.
Finck-Barbançon, V., Prévost, G. & Piémont, Y. (1991). *Res. Microbiol.* **142**, 75–85.
Girgis, D. O., Sloop, G. D., Reed, J. M. & O'Callaghan, R. J. (2005). *Invest. Ophthalmol. Vis. Sci.* **46**, 2064–2070.
Gouaux, J. E., Braha, O., Hobaugh, M. R., Song, L., Cheley, S., Shustak, C. & Bayley, H. (1994). *Proc. Natl Acad. Sci. USA*, **91**, 12828–12831.
Gravet, A., Colin, D. A., Keller, D., Girardot, R., Monteil, H., Prévost, G. & Giradot, R. (1998). *FEBS Lett.* **436**, 202–208.
Gravet, A., Couppié, P., Meunier, O., Clyti, E., Moreau, B., Pradinaud, R., Monteil, H. & Prévost, G. (2001). *J. Clin. Microbiol.* **39**, 4349–4356.
Gravet, A., Rondeau, M., Harf-Monteil, C., Grunenberger, F., Monteil, H., Scheftel, J.-M. & Prévost, G. (1999). *J. Clin. Microbiol.* **37**, 4012–4019.
Gray, G. S. & Kehoe, M. (1984). *Infect. Immun.* **46**, 615–618.
Guillet, V., Roblin, P., Werner, S., Coraiola, M., Menestrina, G., Monteil, H., Prévost, G. & Mourey, L. (2004). *J. Biol. Chem.* **279**, 41028–41037.
Joubert, O., Viero, G., Keller, D., Martinez, E., Colin, D. A., Monteil, H., Mourey, L., Dalla Serra, M. & Prévost, G. (2006). *Biochem. J.* **396**, 381–389.
Kabsch, W. (2010). *Acta Cryst.* D**66**, 125–132.
Kaneko, J., Muramoto, K. & Kamio, Y. (1997). *Biosci. Biotechnol. Biochem.* **61**, 541–544.
Kantardjieff, K. A. & Rupp, B. (2003). *Protein Sci.* **12**, 1865–1871.
Lina, G., Piémont, Y., Godail-Gamot, F., Bes, M., Peter, M. O., Gauduchon, V., Vandenesch, F. & Etienne, J. (1999). *Clin. Infect. Dis.* **29**, 1128–1132.
McCoy, A. J., Grosse-Kunstleve, R. W., Adams, P. D., Winn, M. D., Storoni, L. C. & Read, R. J. (2007). *J. Appl. Cryst.* **40**, 658–674.
Meyer, F., Girardot, R., Piémont, Y., Prévost, G. & Colin, D. A. (2009). *Infect. Immun.* **77**, 266–273.
Morinaga, N., Kaihou, Y. & Noda, M. (2003). *Microbiol. Immunol.* **47**, 81–90.
Olson, R., Nariya, H., Yokota, K., Kamio, Y. & Gouaux, E. (1999). *Nature Struct. Biol.* **6**, 134–140.
Pédelacq, J.-D., Maveyraud, L., Prévost, G., Baba-Moussa, L., González, A., Courcelle, E., Shepard, W., Monteil, H., Samama, J.-P. & Mourey, L. (1999). *Structure*, **7**, 277–287.
Prévost, G., Bouakham, T., Piémont, Y. & Monteil, H. (1995). *FEBS Lett.* **376**, 135–140.
Prévost, G., Couppié, P., Prévost, P., Gayet, S., Petiau, P., Cribier, B., Monteil, H. & Piémont, Y. (1995). *J. Med. Microbiol.* **42**, 237–245.
Prévost, G., Cribier, B., Couppié, P., Petiau, P., Supersac, G., Finck-Barbancon, V., Monteil, H. & Piémont, Y. (1995). *Infect. Immun.* **63**, 4121–4129.
Roblin, P., Guillet, V., Joubert, O., Keller, D., Erard, M., Maveyraud, L., Prévost, G. & Mourey, L. (2008). *Proteins*, **71**, 485–496.
Song, L., Hobaugh, M. R., Shustak, C., Cheley, S., Bayley, H. & Gouaux, J. E. (1996). *Science*, **274**, 1859–1866.
Supersac, G., Piémont, Y., Kubina, M., Prévost, G. & Foster, T. J. (1998). *Microb. Pathog.* **24**, 241–251.
Tseng, C. W., Kyme, P., Low, J., Rocha, M. A., Alsabeh, R., Miller, L. G., Otto, M., Arditi, M., Diep, B. A., Nizet, V., Doherty, T. M., Beenhouwer, D. O. & Liu, G. Y. (2009). *PLoS One*, **4**, e6387.
Ventura, C. L., Malachowa, N., Hammer, C. H., Nardone, G. A., Robinson, M. A., Kobayashi, S. D. & DeLeo, F. R. (2010). *PLoS One*, **5**, e11634.

Viero, G., Cunaccia, R., Prévost, G., Werner, S., Monteil, H., Keller, D., Joubert, O., Menestrina, G. & Dalla Serra, M. (2006). *Biochem. J.* **394**, 217–225.
Vonrhein, C., Flensburg, C., Keller, P., Sharff, A., Smart, O., Paciorek, W., Womack, T. & Bricogne, G. (2011). *Acta Cryst.* D**67**, 293–302.
Winn, M. D. *et al.* (2011). *Acta Cryst.* D**67**, 235–242.
Woodin, A. M. (1960). *Biochem. J.* **75**, 158–165.
Yamashita, K., Kawai, Y., Tanaka, Y., Hirano, N., Kaneko, J., Tomita, N., Ohta, M., Kamio, Y., Yao, M. & Tanaka, I. (2011). *Proc. Natl Acad. Sci. USA*, **108**, 17314–17319.